energies

MDPI

Article

Optimized Demand Side Management for Refrigeration: Modeling and Case Study Insights from Kenya

Josephine Nakato Kakande [1,2], Godiana Hagile Philipo [1,3] and Stefan Krauter [1,*]

[1] Chair of Electrical Energy Technology—Sustainable Energy Concepts (EET-NEK), Faculty of Computer Science, Electrical Engineering and Mathematics, Paderborn University, Pohlweg 55, 33098 Paderborn, Germany; jkakande@mail.uni-paderborn.de (J.N.K.); philipog@campus.uni-paderborn.de (G.H.P.)
[2] Department of Electrical and Computer Engineering, Makerere University, Kampala P.O. Box 7062, Uganda
[3] Department of Material, Energy, Water and Environmental Sciences, The Nelson Mandela African Institution of Science and Technology, Arusha P.O. Box 447, Tanzania
* Correspondence: stefan.krauter@uni-paderborn.de

Abstract

According to the International Institute of Refrigeration (IIR), 20% of worldwide electricity consumption is for refrigeration, with domestic refrigeration appliances comprising a fifth of this demand. As the uptake of renewable energy sources for on-grid and isolated electricity supply increases, the need for mechanisms to match demand and supply better and increase power system flexibility has led to enhanced attention on demand-side management (DSM) practices to boost technology, infrastructure, and market efficiencies. Refrigeration requirements will continue to rise with development and climate change. In this work, particle swarm optimization (PSO) is used to evaluate energy saving and load factor improvement possibilities for refrigeration devices at a site in Kenya, using a combination of DSM load shifting and strategic conservation, and based on appliance temperature evolution measurements. Refrigeration energy savings of up to 18% are obtained, and the load factor is reduced. Modeling is done for a hybrid system with grid, solar PV, and battery, showing a marginal increase in solar energy supply to the load relative to the no DSM case, while the grid portion of the load supply reduces by almost 25% for DSM relative to No DSM.

Keywords: refrigeration; demand-side management; PSO; solar; battery; grid; temperature measurements; load shifting; strategic conservation

check for updates

Academic Editor: Maksymilian Kochanski

Received: 18 April 2025
Revised: 16 June 2025
Accepted: 18 June 2025
Published: 21 June 2025

Citation: Kakande, J.N.; Philipo, G.H.; Krauter, S. Optimized Demand Side Management for Refrigeration: Modeling and Case Study Insights from Kenya. *Energies* **2025**, *18*, 3258. https://doi.org/10.3390/en18133258

Copyright: © 2025 by the authors. Licensee MDPI, Basel, Switzerland. This article is an open access article distributed under the terms and conditions of the Creative Commons Attribution (CC BY) license (https://creativecommons.org/licenses/by/4.0/).

1. Introduction

Globally, 20% of electricity usage is for refrigeration applications, with 20% of this attributed to domestic freezers and fridges [1]. In Africa, the number of refrigeration appliances has been predicted to rise by 250% to 200 million by 2030 [2]. The number of residential refrigeration appliances in Kenya alone was projected to increase from almost 3.5 million in 2023 to 6 million by 2030 [3]. In addition, renewable energy solutions and decentralized energy systems are providing an increasingly important means of bridging the electricity access gap.

Demand-side management (DSM) typically aims to modify electricity consumption by adjusting usage to periods when electricity demand and/or prices are low, thus increasing efficiencies and reducing costs. Refrigeration loads provide a suitable scope for demand management because of the inherent thermal inertia capabilities they possess that facilitate

load shifting and power and energy consumption modulation [4]. Their relatively stable but potentially flexible demand patterns offer a means to match intermittent renewable energy sources better.

Approaches for energy optimization include mathematical programming-based approaches such as convex programming, quadratic programming (QP), mixed-integer linear programming (MILP), mixed-integer nonlinear programming (MINLP) and linear programming [5]. In the literature, binary linear programming [6] and model predictive control (MPC) with binary quadratic programming [7] for appliance management and scheduling are discussed. Such mathematical programming-based approaches are, however, ill-equipped to handle scenarios of numerous controllable devices with varying consumption patterns and specifications, and computation takes long [8,9].

Metaheuristic optimization algorithms such as particle swarm optimization (PSO), genetic algorithms (GAs) and ant colony algorithms belong to a class of optimization methods which use populations that search through a search space for a near-optimal solution [10]. These three methods belong to the category of nature-inspired methods. Several studies have been conducted evaluating the use of GAs and PSOs for load management applications. In [11], the use of GA for appliance scheduling in a smart grid with commercial, residential, and industrial customers is presented. Energy and cost savings, as well as peak demand reduction, are achieved relative to the no-DSM scenario. However, the GA method requires significant computational resources and time. PSO-based approaches are presented in [9,12], and the PSO performance is compared with the grasshopper optimization algorithm (GOA) [13]. Another nature-based approach, the hybrid WFS2ACSO technique based on combining the wingsuit flying search algorithm (WFSA) and artificial cell swarm optimization (ACSO) is presented in [14]. The aforementioned references utilize varying hourly tariffs and an objective function that seeks to minimize bills and hence is inversely proportional to the hourly price.

In [15], two-stage optimization is used for load shifting with the objective of minimizing energy costs and maximizing user comfort in a grid connected system with renewable generation. Reduction of energy costs while keeping power below the maximum demand limit were the objectives for the hybrid energy system described in [16]. Customer comfort is considered in the control of aggregated thermostatically controlled loads in [17], whereby heterogeneous air conditioners are clustered using Markov chains.

A study of load management for refrigeration in Mannheim, Germany, recommended commercial food-retailing (such as by supermarkets) and hotels plus restaurants as best suited for demand management, and cited at least 4% savings in peak demand as being possible in Germany [4]. In [18], the use of ice for thermal storage in an Italian supermarket with a heat pump and varying electricity tariffs shows significant long-term cost savings.

Adjusting loads through load shifting changes the timing of energy use but does not always lower the appliances' total energy consumption. This occurs because any decrease in usage during certain periods is usually balanced by an increase before or after, known as load recovery. The duration of these adjustments depends on the specific properties of the load [19]. Some prior studies have assumed an aggregated fraction of the load is shifted without considering the particulars of the load, e.g., 20% [20], or up to 20% [21]. However, the food safety constraints for refrigeration appliances necessitate additional constraint considerations beyond basic load shifting.

In this work, an optimization approach for demand side management of refrigeration appliances in an on-grid setting and based on experimental data for a residential site in Lwak, Kenya is proposed to attain a redistributed energy profile and lower electricity usage and hence energy costs, but still meet food safety temperature requirements. The proposed

method incorporates the use of appliance temperature evolution measurements and PSO to achieve load shifting using refrigeration loads and reduced energy demand.

Prior studies utilize time-of-use (TOU) tariffs to minimize costs [11,12]. However, since Kenya utilizes a constant tariff for domestic customers, an objective function based on the average daily power is used to schedule the fridges and freezers and hence modulate the load profile. PSO is used because it can be applied in scenarios where multiple loads and consumers are being considered, for example for direct load control (DLC) for many customers of a microgrid or the grid.

Our proposed approach uses a combination of load shifting and strategic conservation to minimize refrigeration energy requirements by considering demand control of several refrigeration appliances.

2. Particle Swarm Optimization

Particle swarm optimization (PSO) is a metaheuristic optimization method designed to imitate the migratory behavior of a school of fish or a flock of birds, which work in combination to achieve a certain objective. It involves communication and continual learning in order for a sufficiently good solution to be arrived at from all solutions possible within a given search space. It can solve discrete, binary, constrained, combinatorial, and multi-objective optimization.

The main algorithm parameters utilized are velocity and position. The exploration stage involves initialization of the swarm parameters, followed by an exploitation stage where the velocity and position change over a number of iterations. The population exists within a search space of possible solutions. The convergence or termination criterion is either the stipulated maximum number of iterations or attaining an output that is sufficiently close to the desired result. Upon fulfilling the criterion for stopping, the best particle so far is chosen as the near-optimal solution [22].

The individual and global best position and cost are stored at each evaluation and used to update the position and velocity of the particles as per Equations (1) and (2).

$$x_i\,(t+1) = x_i\,(t) + v_i\,(t+1) \tag{1}$$

$$v_i\,(t+1) = w\;\; v_i\,(t) + \varphi_1\, c_1\,(P_{i_{best}} - x_i\,(t)) + \varphi_2\, c_2\,\left(P_{g_{best}} - x_i\,(t)\right) \tag{2}$$

where i is particle's number ($i = 1, \ldots, N$; N being the number of particles in the swarm), $x_i\,(t+1)$ and $x_i\,(t)$ are vectors describing the next and current positions of each particle, respectively, and the velocity vector $v_i\,(t+1)$ indicates the next movement direction of each particle in the population [10,22]. $v_i\,(t)$ is restricted to the range $[-v_{max}, v_{max}]$. If maximum velocity v_{max}, is excessively large, it widens the exploration range; however, if it is excessively small, particles will tend to prioritize local search.

The inertia weight w determines the balance between the exploratory and exploitation stages. As exploitation progresses, the exploration scope should decrease such that particles shift from searching the wide space to fine tuning upon entering a good location [22]. When the inertia weight w is large, it promotes global search by allowing particles to explore a wider search space. Conversely, a small inertia weight w promotes local search by focusing particles on exploiting local regions of the search space. Hence, w is updated as shown in Equation (3).

$$w = w_{min} + (w_{max} - w_{min}) \cdot \left(\frac{iter_{max} - iter}{iter_{max}}\right) \tag{3}$$

where w_{max} represents the predefined maximum value of w, while w_{min} represents the predefined minimum value, usually 0.9 and 0.4, respectively. Parameters $iter$ and $iter_{max}$

refer to the current iteration of the algorithm and the maximum number of iterations respectively [12,23].

P_{ibest} and P_{gbest} respectively indicate the personal best position attained thus far by each particle and the global best position from the entire population. φ_1 and φ_2 are random independent numbers in the range [0, 1], while c_1 and c_2 are the cognitive acceleration constant and the social acceleration constant, respectively. The acceleration constants control the effect of the best positions and typically sum up to 4. Usually, static values of c_1 and c_2 are used and most commonly $c_1 = c_2$.

Among the advantages of PSO relative to similar nature-inspired algorithms are [10,24]:

- It is able to reach a near-optimal solution with simpler implementation and less computational requirements than other heuristic algorithms, e.g., GAs.
- It needs fewer parameters for tuning adjustments.
- PSO uses historical memory of all particles in searching, unlike GAs which cannot harness historical memory because they change the population in each generation, replacing the old population with a newer and more efficient one.
- High applicability since it is less sensitive to the nature of the objective function and can be used for varying optimization problems. PSO can be used to optimize large dimensional problems.

For this work, the PSO approach in [9,12] is developed further for refrigeration devices and constant tariff situations, having considered internal appliance temperature evolution.

3. Methods and Materials

3.1. Site and System Description

The site, which is described in [25], has three buildings and was powered by the main grid with a 40 kW diesel generator for backup supply to it and neighboring buildings. Power measurements for the three buildings for the period from 6 February to 10 February 2023 were used for the PSO-based load shifting. The 24 hour average load profile described in [25] was used for 24 hour DSM (involving strategic conservation and load shifting) using PSO.

3.2. Appliance Measurement Setup

The suggested temperature range for refrigerators to prevent food spoilage is typically 2 °C to 6 °C [26]. Temperature thresholds of 5 °C to 8 °C for refrigerators have been proposed [27]. On the other hand, the generally recommended temperature for freezers is below −12 °C [28] or, more commonly, below −18 °C [29].

To monitor internal temperatures for the eight refrigeration appliances at the site in Lwak, AM2302 sensors were interfaced with Raspberry Pi 3 Model B microcontrollers, which facilitated data logging. Power usage and operational control of the appliances were managed using Edimax SP-2101W V3 smart plugs, which support remote switching functionality. Power data was logged using the Edismart App and the open-source Tesseract OCR (optical character recognition) engine in Python 3.8.10 [25]. The appliance details, as described in [25], are shown in Table 1.

Table 1. Refrigeration appliance details.

Appliance	Description	Average Measured Power (W)
Freezer 1	Bruhm BCF-398SD	123
Fridge 2	Toshiba GR-EF 33	174
Freezer 3	HTCF208A2	133
Fridge 5	Haier	62
Freezer 6	ArmCoAF-C38(K)	112
Fridge 8	Goldstar GR-312S	132
Freezer 9	-	204
Freezer 10	Bruhm BCF-398SD	114

From the freezer measurements, it was found that internal temperatures could remain within an 8 °C temperature band when the appliances are switched off for 3 to 4 hours, or even up to 7 hours for Freezer 6 [25]. The off period can be lengthened by increasing the thermal mass of the fridge contents, e.g., with phase change materials or water, by lowering the thermostat temperature settings so that the off state begins at a lower temperature, by reducing the frequency and duration of the appliance door opening, or by improving the device insulation properties.

Based on those measurements and findings, a conservative load switching cycle of 4 hours on and 2 hours off is proposed for the DSM of Freezer 6, while the other appliances utilize a 5:1 hourly ON:OFF cycle as it is assumed that the other seven appliances have lower thermal inertia and hence require longer on periods for food safety (see Table 2). It is also assumed that the forecasted load for the next 24 hours is perfectly known [12], which could be possible if predictive forecasting is incorporated [20].

Table 2. Refrigeration appliance control cases.

Parameter	Freezer 1, Fridge 2, Freezer 3, Fridge 5, Fridge 8, Freezer 9, Freezer 10	Freezer 6
Switching cycle	5:1 hourly ON:OFF cycle over 24 hours	4:2 hourly ON:OFF cycle over 24 hours

As a 24-hour period is split into 6-hour periods and it is assumed that within every 6-hour slot Freezer 6 will be off for two hours, even if for two 6-hour adjacent slots the off periods are successively the last two hours and first two hours, the consecutive off time will be only 4 hours which would be within the desired food safety temperature considerations for Freezer 6 based on the measurements described in [25].

It should be noted that the effects of user interactions, thermal mass, and ambient temperature have not been considered in this analysis.

3.3. PSO Algorithm Description

The target curve $Targ_h$ is specified as the average of the forecasted hourly power; the forecasted load is the load profile values in Figure 1 [25].

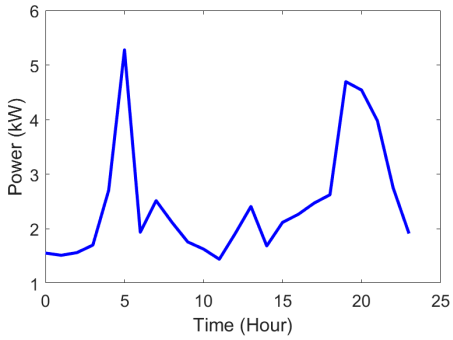

Figure 1. Average hourly maximum power demand at Lwak from 6 to 10 February 2023.

Equation (4) was chosen as the target curve as the grid tariff is constant, and so price-based optimization was not viable.

$$Targ_h = \frac{\sum_{h=1}^{H=24} \left(load_{fc_h} \right)}{H} \tag{4}$$

where $Targ_h$ is the hourly target load power and $load_{fc_h}$ represents the forecasted load at hour h of the day's $H = 24$ hours.

The non-shiftable loads are handled as a single aggregated time varying load [15,16].

The reducible load margin (RLM) is calculated as the difference between the forecasted load and the target for each hour:

$$RLM_h = load_{fc_h} - Targ_h \tag{5}$$

The marginal load adjustment is determined based on whether the forecasted load is greater than or less than the target load. Positive RLM values indicate a need for load reduction through device disconnections, while negative values indicate a need for load addition through device connections.

An objective function f_h is constructed to derive a modified final load curve that minimizes the difference between the RLM and the load change $\Delta load_h$ at each time step:

$$\text{Minimize}: \ f_h = [\ |RLM_h| - |\Delta load_h|\ ] \tag{6}$$

The constraint is that the number of devices shifted in any hour must not exceed the number of devices available for shifting in that hour.

RLM_h is the desirable change in load (increase or decrease) that would modify the load curve to the target $Targ_h$ but it cannot be achieved exactly, so f_h tries to ensure the change in load $\Delta load_h$ is as close as possible to RLM_h.

$$\Delta load_h = connect\ (h) - disconnect\ (h) \tag{7}$$

where $connect\ (h)$ denotes the loads connected at hour h and $disconnect\ (h)$ the loads disconnected at hour h.

$$connect(h) = \sum_{d=1}^{N_d} \sum_{m=1}^{g_d} \sum_{l=1}^{h-1} X_{dl(h-m+1)}\ P_{md} \tag{8}$$

computes the power at hour h due to devices that were shifted to start at earlier times l, such that h is their mth hour of operation. d denotes the types of devices, N_d is the total number of types of devices, m is the hour of operation of device d, g_d is the operation duration (in hours) of device type d, and P_{md} denotes power consumption for device type d

in its mth hour of operation. X_{dlh}, the decision variable, denotes the number of devices of type d shifted to start earlier from hour l to h.

$$disconnect(h) = \sum_{d=1}^{N_d} \sum_{m=1}^{g_d} \sum_{q=h+1}^{h+s_d} X_{d(h-m+1)q} \, P_{md} \tag{9}$$

sums up the power that would have existed at hour h as the mth hour of operation for devices that would have started running at $(h - m + 1)$, but were shifted later or delayed to start at time q. s_d is the maximum number of hours device d can be delayed [14] while still completing its operation within its allowed window $[B_d, E_d]$, where B_d is the earliest time device d can start running and E_d is the latest time device d can finish running.

The constraints include the following.

Maximum shifting delay for device d should not exceed s_d hours,

$$X_{dhq} = 0, \text{for } \; q < h \;\; \text{and} \;\; q > h + s_d \tag{10}$$

At any hour h, the number of devices of type d being either connected or disconnected must not exceed those available for control A_{dh} in that hour.

$$X_{dh} \leq A_{dh} \tag{11}$$

The number of devices for shifting must be non-negative.

$$X_{dh} \geq 0 \tag{12}$$

This information is used to decide whether to connect or disconnect the load at each time step, with the aim of bringing the load curve closer to the target curve [9].

The simulation was carried out with MATLAB 2023. A uniform electricity price p = 0.18 USD/kWh for Kenya's domestic grid customers [30] is used in the cost computations. The maximum number of iterations $iter_{max}$ = 100, w ranges from 0.4 to 0.9, $c_1 = c_2$ = 2. φ_1 and φ_2 are between 0 and 1 [27]. The swarm population N = 100.

4. PSO-Based Load Shifting Results

Customer comfort as an objective in the control of thermostatically controlled loads (TCLs) is discussed in [17]. Regulation of autonomous microgrid frequency using decentralized control of refrigerators in tandem with an ESS is shown to reduce ESS capacity requirements when user comfort and customer participation are taken into account. Customer comfort is low when the frequency deviation is large, as it implies a big temperature change [31].

In this work, it is assumed that the customer comfort is not affected by the appliance's on-time curtailment as the proposed off-durations are taken as short enough to keep internal temperatures within the required bounds for food safety.

Load shifting was simulated to modify the load profile for a grid-connected residential site in Kenya by controlling eight refrigeration appliances as the shiftable devices, and with operational times specified based on the temperature measurements described in [25].

Unlike [32], where the staggering is achieved by cumulatively incrementing the number of refrigeration devices to which the control strategy is applied during the control modification window, in our work staggering is not applied in a temporally graded manner.

The load profiles incorporating energy savings due to curtailing the fridge and freezer on times (strategic load conservation) and implementing load shifting are shown in

Figure 2. The curtailment is because the total refrigeration energy has been reduced since the appliances are switched off for some hours, as described in Table 2. Table 3 summarizes the results of the proposed strategic conservation and load shifting algorithm.

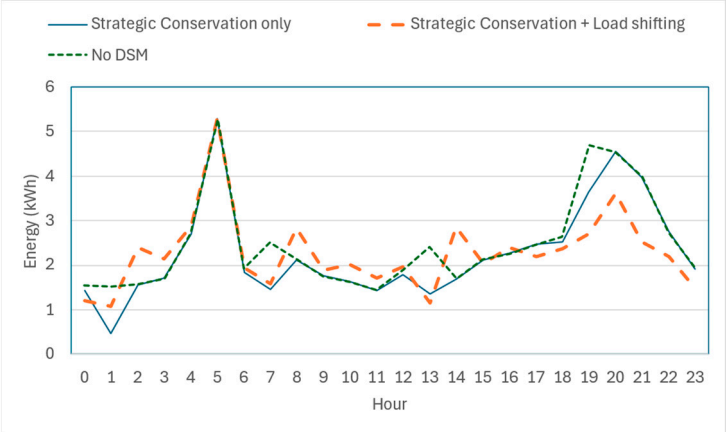

Figure 2. Load profiles for the No DSM case (dotted line) and DSM case with refrigeration curtailment (strategic conservation) and load shifting (long dashed line).

Table 3. Results from PSO optimized load shifting of refrigeration appliances.

Parameter	No DSM	Strategic Conservation Only	DSM (Strategic Conservation and Load Shifting)
Total daily energy (kWh)	59.11	54.45	54.45
Minimum daily energy (kWh)	1.44	0.46	1.09
Peak daily load (kW)	5.28	5.28	5.28
Peak hour daily (hour)	5	5	5
Average daily load (kW)	2.46	2.27	2.27
Peak evening load (kW)	4.70	4.54	3.61
Peak evening hour (hour)	19	20	20
Load Factor (Average to Peak ratio)	0.47	0.43	0.43
Reduction in daily refrigeration energy (%)		18%	18%
Reduction in refrigeration energy annual cost (USD/year)		306	306
Overall reduction in total daily energy (%)		8%	8%

The average load reduces from 2.46 kW to 2.27 kW when strategic conservation and load shifting are applied, as shown in Table 3. The load factor declines by 8.5% from 0.47 to 0.43 when DSM is introduced. This fairly small decline in load factor is due to the dual peak load profile shape for this particular site, which means that there is not much leeway for load shifting, particularly in the morning hours. The morning peak remains unchanged because of the relatively small load shifting time windows and because the number of shiftable devices is few; having a bigger number of shiftable devices and shiftable device types increases the load shifting potential and gains, as in [12]. With DSM, the evening peak occurs an hour later than for the no DSM case, around 20:00 hrs.

An increase in load factor would translate to cost efficiencies since the infrastructure is utilized more efficiently, and, hence, infrastructure and component upgrades and investments to meet peak load can be deferred. In a microgrid scenario where there are many loads that display the more typical "duck curve" [33], an improved load factor may be possible.

The evening peak decreases by only 3% when only strategic conservation is applied, but shows a more significant 23% peak reduction for a combination of strategic conservation and load shifting relative to the No DSM scenario. The daily refrigeration energy does decrease by a significant 18% due to the appliance's on-off pattern (strategic conservation) specified in Table 2, and the overall decrease in demand is 8%.

In general, the longer the shifting period permitted, e.g., 48 hours rather than 24 hours, the higher the possible flexibility benefits and savings from load shifting. To achieve greater control and load shifting benefits, smaller time steps could also be used, e.g., 15-min intervals rather than hourly intervals.

The application of DSM control to other and more types of deferrable electrical devices would likely yield better load factor improvements.

Next, using the results from the proposed load shifting and strategic conservation DSM approach, the modeling of a hybrid solar PV system with battery storage is carried out, and the results are presented in the next section.

5. Refrigeration DSM Modeling for a Hybrid PV System with Battery Storage

A PV system with storage was planned for installation at the site in Lwak with the following specifications:

- 12.45 kWp solar PV system with 30 JA Solar JAM72S10-415W solar PV modules, connected to 3 SMA Sunny Boy 5.0 inverters.
- 37.58 kWh battery energy storage system (BESS) with 36 Hoppecke Sun power VR M 12-105 lead acid batteries, connected to 3 SMA Sunny Island 8.0H-13 inverters.

The general system topology is shown in Figure 3. The AC loads comprise the base (non-shiftable) loads and shiftable loads (refrigeration appliances). Grid reliability is assumed to be 100%, such that there is no loss of load, and hence, the shared generator is ignored.

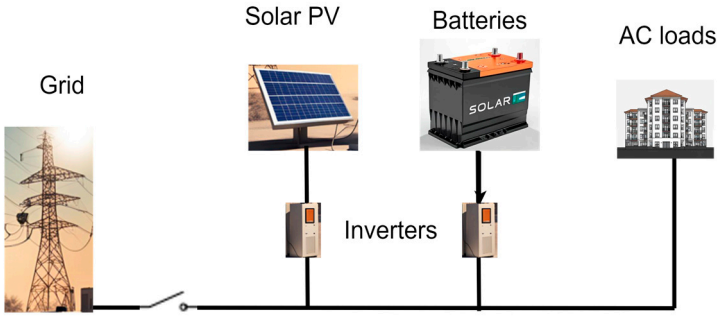

Figure 3. Schematic of the proposed hybrid energy system at Lwak.

The 24-hour load profile data without DSM [25] and with PSO-based DSM (involving strategic conservation and load shifting) shown in Figure 2 were used for modeling.

The system was modeled in MATLAB 2023 for the day with the lowest irradiance and hence lowest PV generation in 2022, using 2022 data of hourly irradiance and temperature for the Lwak site obtained from the NASA (National Aeronautics and Space Administration) website [34]. The minimum and maximum battery state of charge (SOC) were set to 50% and 100%, respectively.

PV production is given by:

$$P_{PV}(t) = P_r \, f_d \, \frac{G(t)}{G_{ref}} \left[1 + K_T \left(T_c - T_{ref}\right)\right] \tag{13}$$

$$T_c = T_{amb} + 0.0256\, G(t) \tag{14}$$

where P_{PV} is the PV-generated power (kW), P_r is the rated PV capacity under standard test conditions (STC) in kW, f_d = 0.9 is the derating factor [35], $G(t)$ and G_{ref} are the incident solar radiation in kW/m^2 and at STC of 1 kW/m^{2,} respectively, the temperature coefficient of power K_T = −0.0037/°C, T_c, T_{ref} = 25 °C and T_{amb} are the cell temperature, reference temperature and ambient temperature respectively, in °C.

The battery equations for charging (Equation (15)) and discharging (Equation (16)) are [36]:

$$E_B(t) = E_B(t-1) + \left(E_G(t) - \frac{E_L(t)}{\eta_{conv}}\right)\eta_{bat}\eta_{ch} \tag{15}$$

$$E_B(t) = E_B(t-1) + \left(E_G(t) - \frac{E_L(t)}{\eta_{conv}}\right)/\eta_{bat}\eta_{disch} \tag{16}$$

where

$$E_G(t) = P_{PV}(t)\,\eta_{conv} \tag{17}$$

$E_B(t)$ is battery energy at time t, E_G denotes PV AC energy, E_L denotes the load energy, η_{conv} is converter efficiency, η_{ch} is battery charging efficiency, η_{disch} is battery discharging efficiency and η_{bat} is battery inverter efficiency.

The constraints include

$$P_G(t) + P_{Grid}(t) = P_L(t) + P_{Bat}(t) \tag{18}$$

$$E_{Bmin} < E_B(t) < E_{Bmax} \tag{19}$$

where P_L is load power (kW), P_{Grid} is grid power (kW) supplied to the load at time t, E_{Bmin} and E_{Bmax} are battery minimum and maximum energy respectively. Battery power P_{Bat} (kW) is positive when charging and negative when discharging. $P_G(t)$ is PV AC power (kW).

The parameters used in the model are summarized in Table 4.

Table 4. System parameters for Lwak hybrid PV and battery system [30,35,37,38].

Component	Parameter	Value	Parameter	Value
PV	PV module rating	0.415 kWp	Derating factor	0.9
	PV capacity	12.45 kWp		
Battery	Nominal capacity	87 Ah	Charging efficiency	98%
	Nominal voltage	12 V	Discharging efficiency	98%
	System DC voltage	48 V	Minimum SOC (%)	50%
	System storage capacity	37.584 kWh	Maximum SOC (%)	100%
			Initial battery SOC (%)	50%
Converter	Power rating	15 kW	Efficiency	96%
	Battery inverter efficiency	96%		
Grid	Tariff	0.18 USD/kWh		

The dispatch algorithm, depicted in Figure 4, is such that priority is given to meeting the load using PV generation. Excess PV energy is used to charge the batteries if the battery state of charge (SOC) is less than 100%. Surplus PV generation above the load and battery charging requirements is curtailed. If there is a deficit in PV energy available to meet the demand, and the battery SOC > 50%, then the battery discharges to meet the load. If the battery energy is insufficient, then the grid supplies the unmet demand.

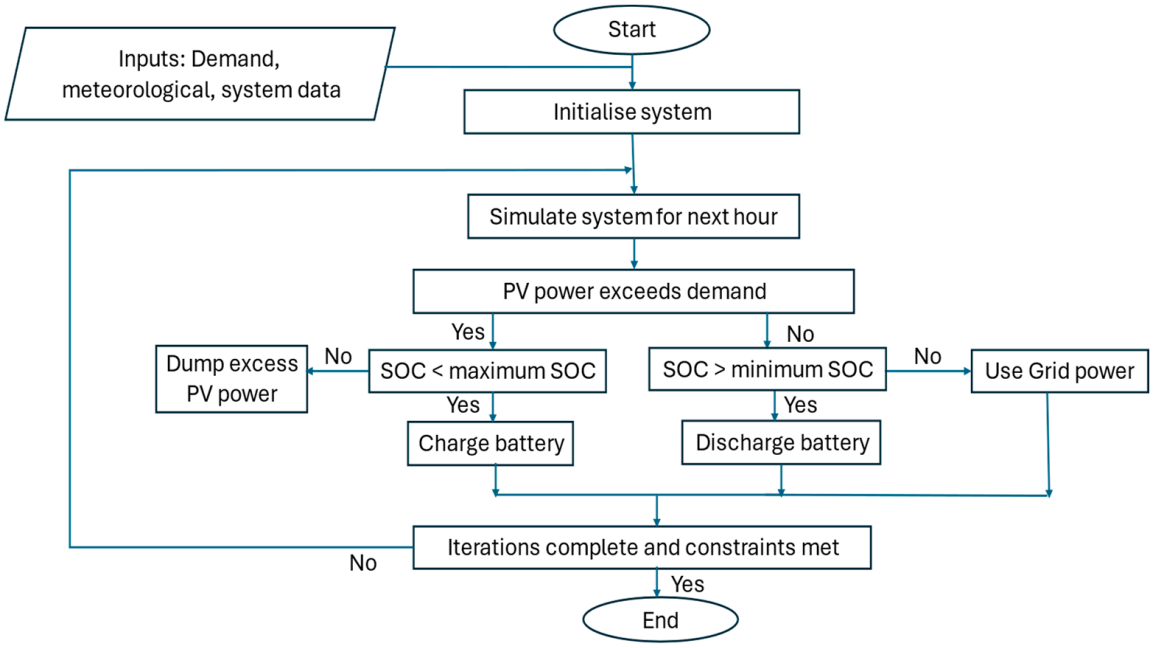

Figure 4. Dispatch algorithm for the hybrid system at Lwak.

Two scenarios were modeled:

- Scenario 1: No DSM + PV + battery storage + grid
- Scenario 2: DSM + PV + battery storage + grid

6. Results for Hybrid System Modeling

Figure 5 shows the plot of PV generation against load for the No DSM and DSM cases.

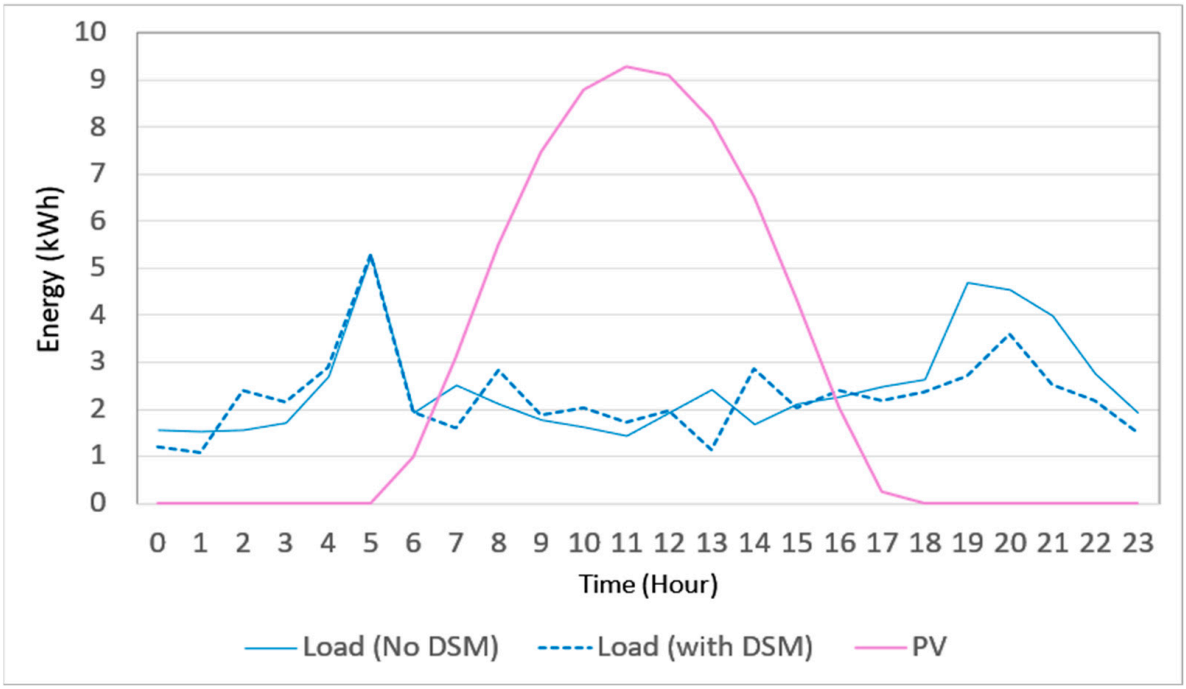

Figure 5. Load profiles without and with DSM and PV energy (kWh for each hour of the day, averaged).

The maximum possible hourly PV generation is 9.29 kWh, and the daily PV energy production is 65.53 kWh, as shown in Table 5. Only 20.88 kWh and 21.31 kWh of the PV

energy is supplied to the No DSM loads and DSM loads, respectively, corresponding to a third of the PV generation. There is a significant PV energy surplus from 12 noon to 3 p.m. for the No DSM case and the DSM case, as shown in Figures 6 and 7, respectively. This surplus could be used for electric cooking, electric water heating, water pumping or e-mobility applications instead of being curtailed.

Table 5. Results from modeling of the DSM for the hybrid system at Lwak.

Parameter	No DSM	DSM
Average daily demand (kWh)	2.46	2.27
Minimum daily demand (kWh)	1.44	1.09
Maximum daily demand (kWh)	5.28	5.28
Total daily demand (kWh)	59.11	54.45
Total annual demand (kWh)	21,576.24	19,874.00
Total daily grid energy (kWh)	20.87	16.34
Grid fraction of load supply (%)	35%	30%
Percentage reduction in daily grid energy (%)		22%
Estimated Annual total grid energy (kWh)	7618.21	5963.59
Grid tariff (USD/kWh)	0.18	0.18
Estimated annual grid energy cost (USD)	1371	1073
Reduction in annual grid energy cost (USD)		297.88
Total daily PV production (kWh)	65.53	65.53
Total PV energy supplied daily to load (kWh)	20.88	21.31
Percentage of PV in load supply (%)	35%	39%

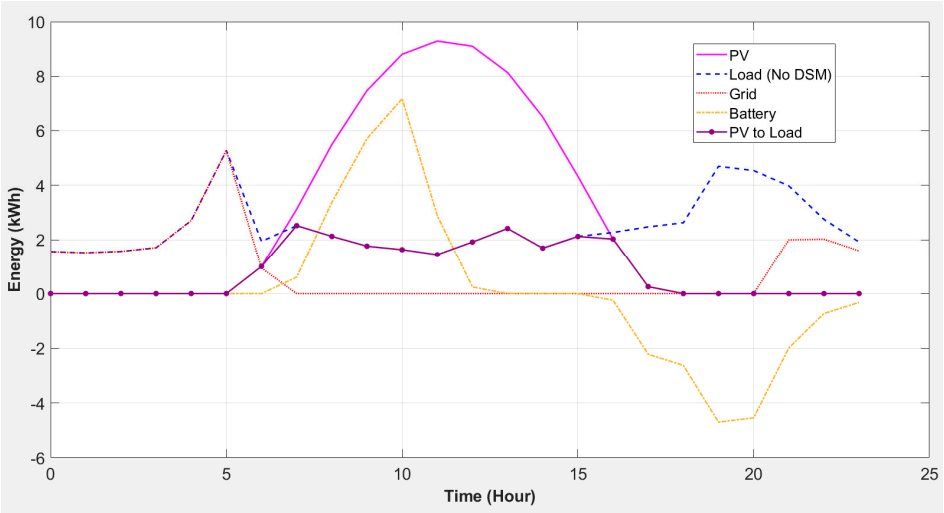

Figure 6. Energy plots for Lwak with no DSM.

With DSM (strategic conservation and load shifting), the portion of daily demand met by the grid reduces from 35% to 30%. This corresponds to an estimated USD 297.88 annual grid energy cost decline with DSM, given the 0.18 USD/kWh Kenya grid tariff [30], and to a 22% reduction in daily grid energy costs. The average lifetime of refrigeration appliances is about 16 years [39]. Assuming 10-year and 15-year operational lifetimes of the refrigeration appliances, estimated conservative grid energy cost savings are about USD 2979 over 10 years and USD 4468 over 15 years, assuming a fixed grid tariff over the years and not considering ageing effects such as insulation degradation. The corresponding estimated energy savings are 16,546 kWh over 10 years and 24,819 kWh over 15 years.

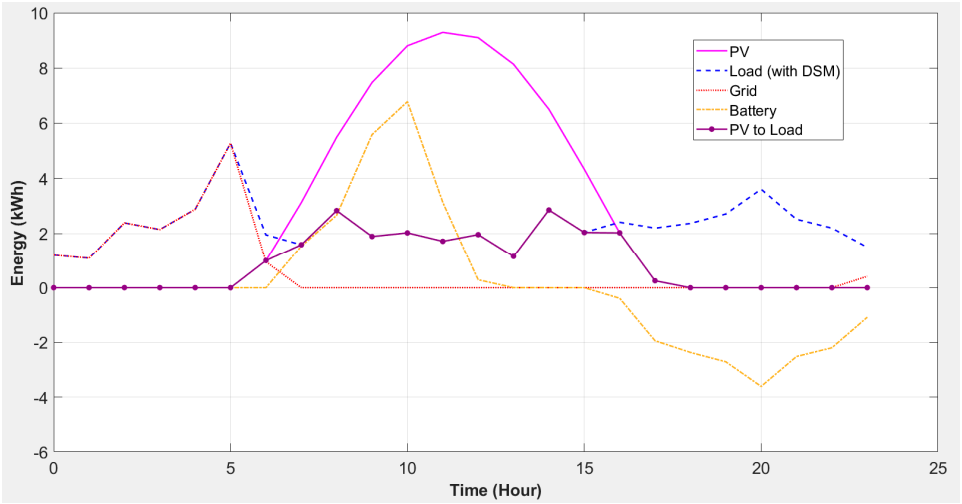

Figure 7. Energy plots for Lwak with DSM.

For the hybrid system, despite the annual demand reducing from 21,576 kWh to 19,874 kWh for the No DSM case relative to the DSM case, there is a 2% increase in the daily PV energy supplying the load for Scenario 2 with DSM compared to the No DSM case (Scenario 1), as shown in Table 5. This marginal 2% increase in PV energy supplied to the DSM load is attributed to the shifting of the DSM refrigeration loads to the PV power generation time period (i.e., the improvement in PV consumption due to load shifting is not large). Better results could probably be attained with a No DSM load profile having a smaller morning peak, more shiftable loads, as well as more granular (smaller) load shifting time steps.

Positive battery energy values in Figures 6 and 7 indicate battery charging, while negative battery energy values indicate battery discharge. The maximum hourly average battery charging power reduces from 7.17 kW to 6.78 kW for No DSM relative to DSM, respectively, while the maximum hourly battery discharging power reduces from 4.70 kW to 3.61 kW for No DSM compared to the DSM case, respectively. The decrease in battery DOD (depth of discharge) given by DOD = 1 − SOC has positive implications and thus benefits for the battery lifetime, whose lifetime is dependent upon DOD, number of cycles, battery temperature [40–42], and ambient temperature [43]. Thus, the proposed DSM would translate to lower battery costs over the system's lifetime compared to No DSM.

Figures 6 and 7 show the hourly average energy for the load profile without DSM and the load profile with refrigeration DSM, respectively, for the day in 2022 with the minimum irradiance as per the 2022 NASA data for the Lwak site. Because of the reduction in evening consumption from DSM, the battery is able to supply the load until as late as 11 p.m. (see Figure 7) and grid power is required from 10 p.m., which is an improvement compared to the No DSM case, whereby grid power imports start as early as 8 p.m. due to the battery discharging faster towards its 50% lower SOC limit (see Figure 6).

7. Conclusions

The use of PSO for load management of refrigeration devices has been presented. After incorporating fridge and freezer on-time curtailment and load shifting, up to 18% reduction in refrigeration energy and thus an 18% drop in refrigeration costs for grid energy are possible for this site. The energy saved can be utilized for applications such as water heating, electric mobility or e-cooking. In Kenya, domestic e-cooking consumes on average 41 kWh per month [30], which is twice the daily energy savings from limiting the refrigerator's on-time. Hence, there is a significant emissions reduction potential due to

transitioning from wood fuel to electricity for cooking. The appliance off period can be extended by increasing the thermal mass of the appliances, for instance with phase change materials, improving the appliance's insulative properties or utilizing more energy-efficient appliances.

Modeling was done for no DSM and DSM of the refrigeration appliances at Lwak using strategic conservation and load shifting for a hybrid PV battery setup with grid supply. With DSM, there was a marginal increase in solar energy supply to the load, while the grid portion of the load supply was reduced by almost a quarter for DSM relative to No DSM.

With longer off times, say due to the use of phase change materials, it is expected that larger energy savings and greater flexibility would be possible. As future work, sensitivity analyses could be conducted, e.g., using different load profiles and irradiance values.

Author Contributions: Conceptualization: J.N.K.; methodology, J.N.K.; software S.K. and J.N.K.; validation, S.K. and J.N.K.; formal analysis, J.N.K.; investigation, J.N.K. and G.H.P.; data curation, S.K. and J.N.K.; writing—original draft preparation, J.N.K.; writing—review and editing, J.N.K., G.H.P. and S.K.; visualization, S.K., J.N.K. and G.H.P.; supervision, S.K.; project administration, S.K.; funding acquisition, S.K. All authors have read and agreed to the published version of the manuscript.

Funding: This research was funded by the German Federal Ministry of Education and Research (BMBF) Project: 03SF0607B Art-D Grids. We acknowledge support for the publication costs by the Open Access Publication Fund of Paderborn University.

Data Availability Statement: Data could be available upon request and agreement from the authorized organizations.

Acknowledgments: The authors are grateful to Lwak Convent for their cooperation.

Conflicts of Interest: The authors declare no conflicts of interest.

Nomenclature

Acronyms

ACSO	Artificial Cell Swarm Optimization
BESS	Battery Energy Storage System
DLC	Direct Load Control
DOD	Depth of Discharge
DSM	Demand Side Management
GA	Genetic algorithm
GOA	Grasshopper Optimization Algorithm
MILP	Mixed-Integer Linear Programming
MINLP	Mixed-Integer Nonlinear Programming
MPC	Model Predictive Control
NASA	National Aeronautics and Space Administration
PSO	Particle Swarm Optimization
PV	Photovoltaic
QP	Quadratic Programming
RLM	Reducible Load Margin
SOC	State of Charge
STC	Standard Test Conditions
TOU	Time-of-Use
USD	United States Dollar
WFSA	Wingsuit Flying Search Algorithm
WFS2ACSO	Wingsuit Flying Search Algorithm and Artificial Cell Swarm Optimization

Symbols

A_{dh}	Devices of type d available for control in hour h
B_d	Earliest time device d can start running
c_1	Cognitive acceleration constant
c_2	Social acceleration constant
$connect(h)$	Shiftable loads connected at hour h
d	Type of device
$disconnect(h)$	Shiftable loads disconnected at hour h
E_B	Battery energy (kWh)
E_{Bmax}	Maximum battery energy (kWh)
E_{Bmin}	Minimum battery energy (kWh)
E_d	Latest time device d can finish running
E_G	PV AC energy (kWh)
E_L	Hourly load energy (kWh)
f_d	Derating factor for PV modules
f_h	Objective function for hour h for PSO algorithm
G	Incident solar radiation (kW/m^2)
g_d	Operation duration of device type d (hours)
G_{ref}	Incident solar radiation at STC (kW/m^2)
h	Hour
H	Number of hours in a day
i	Number of a particle in the swarm population
$iter$	Current iteration
$iter_{max}$	Maximum number of iterations
K_T	Temperature coefficient of power for solar PV modules (/°C)
$load_{fc_h}$	Forecasted load at hour h (kW)
$\Delta load_h$	Change in load at hour h (kW)
N	Number of particles in the swarm population
η_{bat}	Battery inverter efficiency
η_{ch}	Battery charging efficiency
η_{conv}	Converter efficiency
η_{disch}	Battery discharging efficiency
N_d	Total number of types of devices
p	Energy price (USD/kWh)
P_{Bat}	Battery power (kW)
P_G	PV AC power (kW)
$P_{g_{best}}$	Global best position from the entire swarm population
P_{Grid}	Grid power (kW)
φ_1, φ_2	Random independent numbers
P_{ibest}	Personal best position of particle i
P_L	Load power (kW)
P_{md}	Power consumption of device d in its mth hour of operation
P_{PV}	PV generated power (kW)
P_r	Rated PV capacity under standard test conditions (kW)
RLM_h	Reducible load margin at hour h
s_d	Maximum possible delay of device d
t	Time
T_{amb}	Ambient temperature (°C)
$Targ_h$	Hourly target load power (kW)
T_c	Cell temperature (°C)
T_{ref}	Reference temperature (°C)

$v_i\ (t)$	Current velocity vector for particle i
$v_i\ (t+1)$	Next velocity vector for particle i
v_{max}	Maximum value of velocity vector
v_{min}	Minimum value of velocity vector
w	Inertia weight
$x_i\ (t)$	Current position of particle i
$x_i\ (t+1)$	Next position of particle i
X_{dlh}	Number of devices of type d shifted to start from hour l to h

References

1. IIR. *The Role of Refrigeration in the Global Economy (2019). 38th Note on Refrigeration Technologies*; IIR: Paris, France, 2019.
2. IEA. *Africa Energy Outlook 2022*; IEA: Paris, France, 2022.
3. Marambe, G.; Edl, M.; Thwala, M.; Blake, P. Overview of the Market on Refrigerating Appliances and Room Air Conditioners in East and Southern Africa. 2021. Available online: https://united4efficiency.org/wp-content/uploads/2021/04/SADC_EAC_Market-Assessment_Cooling_20210205_Final.pdf (accessed on 28 January 2025).
4. Grein, A.; Pehnt, M. Load Management for Refrigeration Systems: Potentials and Barriers. *Energy Policy* **2011**, *39*, 5598–5608. [CrossRef]
5. Meliani, M.; Barkany, A.E.; Abbassi, I.E.; Darcherif, A.M.; Mahmoudi, M. Energy Management in the Smart Grid: State-of-the-Art and Future Trends. *Int. J. Eng. Bus. Manag.* **2021**, *13*, 1–26. [CrossRef]
6. Jaradat, M.; Jarrah, M.; Jararweh, Y.; Al-Ayyoub, M.; Bousselham, A. Integration of Renewable Energy in Demand-Side Management for Home Appliances. In Proceedings of the 2014 International Renewable and Sustainable Energy Conference (IRSEC), Ouarzazate, Morocco, 17–19 October 2014; pp. 571–576. [CrossRef]
7. Sabegh, M.R.Z.; Bingham, C. Model Predictive Control with Binary Quadratic Programming for the Scheduled Operation of Domestic Refrigerators. *Energies* **2019**, *12*, 4649. [CrossRef]
8. Das, C.K.; Bass, O.; Kothapalli, G.; Mahmoud, T.S.; Habibi, D. Overview of Energy Storage Systems in Distribution Networks: Placement, Sizing, Operation, and Power Quality. *Renew. Sustain. Energy Rev.* **2018**, *91*, 1205–1230. [CrossRef]
9. Banday, Z.; Yadav, P. Demand Side Management in Power Grid Using Particle Swarm Optimization. *Int. J. Sci. Res. Dev.* **2020**, *8*, 817–821.
10. Menos-aikateriniadis, C.; Lamprinos, I.; Georgilakis, P.S. Particle Swarm Optimization in Residential Demand-Side Management: A Review on Scheduling and Control Algorithms for Demand Response Provision. *Energies* **2022**, *15*, 2211. [CrossRef]
11. Logenthiran, T.; Srinivasan, D.; Shun, T.Z. Demand Side Management in Smart Grid Using Heuristic Optimization. *IEEE Trans. Smart Grid* **2012**, *3*, 1244–1252. [CrossRef]
12. Gupta, I.; Anandini, G.N.; Gupta, M. An Hour Wise Device Scheduling Approach for Demand Side Management in Smart Grid Using Particle Swarm Optimization. In Proceedings of the 2016 National Power Systems Conference (NPSC), Bhubaneswar, India, 19–21 December 2016. [CrossRef]
13. Jamil, M.; Mittal, S. Hourly Load Shifting Approach for Demand Side Management in Smart Grid Using Grasshopper Optimisation Algorithm. *IET Gener. Transm. Distrib.* **2020**, *14*, 808–815. [CrossRef]
14. Venkatesh, B.; Sankaramurthy, P.; Chokkalingam, B.; Mihet-popa, L. Managing the Demand in a Micro Grid Based on Load Shifting with Controllable Devices Using Hybrid WFS2ACSO Technique. *Energies* **2022**, *15*, 790. [CrossRef]
15. Bhamidi, L.; Sivasubramani, S. Optimal Sizing of Smart Home Renewable Energy Resources and Battery under Prosumer-Based Energy Management. *IEEE Syst. J.* **2021**, *15*, 105–113. [CrossRef]
16. Arun, S.L.; Selvan, M.P. Intelligent Residential Energy Management System for Dynamic Demand Response in Smart Buildings. *IEEE Syst. J.* **2018**, *12*, 1329–1340. [CrossRef]
17. Lin, S.; Liu, D.; Hu, F.; Li, F.; Dong, W.; Li, D.; Fu, Y. Grouping Control Strategy for Aggregated Thermostatically Controlled Loads. *Electr. Power Syst. Res.* **2019**, *171*, 97–104. [CrossRef]
18. Toffoletti, G.; Cortella, G.; D'Agaro, P. Thermodynamic and Economic Seasonal Analysis of a Transcritical CO_2 Supermarket with HVAC Supply through Ice Thermal Energy Storage (ITES). *J. Clean. Prod.* **2024**, *434*, 139832. [CrossRef]
19. Almenta, M.M.; Morrow, J.; Best, R.; Fox, B. Assessment of Domestic Load Suitable for Smart Consumer Load Participation. In Proceedings of the 2013 48th International Universities' Power Engineering Conference (UPEC), Dublin, Ireland, 2–5 September 2013; IEEE: Piscataway, NJ, USA, 2013; pp. 1–6. [CrossRef]
20. Philipo, G.H.; Kakande, J.N.; Krauter, S. Neural Network-Based Demand-Side Management in a Stand-Alone Solar PV-Battery Microgrid Using Load-Shifting and Peak-Clipping. *Energies* **2022**, *15*, 5215. [CrossRef]

21. Omotoso, H.O.; Al-Shaalan, A.M.; Farh, H.M.H.; Al-Shamma'a, A.A. Techno-Economic Evaluation of Hybrid Energy Systems Using Artificial Ecosystem-Based Optimization with Demand Side Management. *Electronics* **2022**, *11*, 204. [CrossRef]
22. Azlina, N.; Aziz, A.; Aziz, K.A. Particle Swarm Optimization for Constrained and Multiobjective Problems: A Brief Review. In Proceedings of the International Conference on Management and Artificial Intelligence IPEDR, Bali, Indonesia, 1–3 April 2011; Volume 6, pp. 146–150.
23. Chen, H.L.; Yang, B.; Wang, S.J.; Wang, G.; Liu, D.Y.; Li, H.Z.; Liu, W. Bin Towards an Optimal Support Vector Machine Classifier Using a Parallel Particle Swarm Optimization Strategy. *Appl. Math. Comput.* **2014**, *239*, 180–197. [CrossRef]
24. Lee, K.Y.; Park, J. Application of Particle Swarm Optimization to Economic Dispatch Problem: Advantages and Disadvantages. In Proceedings of the 2006 IEEE PES Power Systems Conference and Exposition, Atlanta, GA, USA, 29 October–1 November 2006; IEEE: Piscataway, NJ, USA, 2006; pp. 188–192. [CrossRef]
25. Kakande, J.N.; Philipo, G.H.; Krauter, S. Demand Side Management Potential of Refrigeration Appliances. In Proceedings of the 2023 IEEE PES/IAS PowerAfrica, Marrakech, Morocco, 6–10 November 2023. [CrossRef]
26. Ovca, A.; Skufca, T.; Jev, M. Temperatures and Storage Conditions in Domestic Refrigerators—Slovenian Scenario. *Food Control* **2021**, *123*, 107715. [CrossRef]
27. Zaman, A.U.; Doyle, J. Smart Grid Control: Demand Side Management in Household Refrigerators as a Tool for Load Shifting. *Macalester J. Phys. Astron.* **2022**, *10*, 15. Available online: https://digitalcommons.macalester.edu/mjpa/vol10/iss1/15 (accessed on 26 May 2023).
28. National Environment Agency. *Guidelines on Proper Storage of Food in Refrigerators and Use of Refrigerators*; National Environment Agency: Singapore, 2016. Available online: https://www.nea.gov.sg/docs/default-source/resource/guidelines-on-proper-storage-of-food-in-refrigerators.pdf (accessed on 25 March 2023).
29. Food and Drug Administration (FDA). Are You Storing Food Safely? Available online: https://www.fda.gov/consumers/consumer-updates/are-you-storing-food-safely (accessed on 25 March 2023).
30. EPRA. *Retail Electricity Tariff Review for the 2022/23–2025/26 4th Tariff Control Period (TCP) Effective 1st April 2023*; Energy and Petroleum Regulatory Authority: Nairobi, Kenya, 2023.
31. Qi, Y.; Jia, H.; Mu, Y. Dynamic Frequency Control of Autonomous Microgrid Based on Family-Friendly Controllable Loads. In Proceedings of the 2013 IEEE PES Innovative Smart Grid Technologies Conference (ISGT), Washington, DC, USA, 24–27 February 2013. [CrossRef]
32. Almenta, M.M.; Morrow, J.; Best, R.; Fox, B.; Foley, A. An Aggregated Fridge-Freezer Peak Shaving and Valley Filling Control Strategy for Enhanced Grid Operations. In Proceedings of the 2015 IEEE Power and Energy Society General Meeting, Denver, CO, USA, 26–30 July 2015; IEEE: Piscataway, NJ, USA, 2015; pp. 1–5. [CrossRef]
33. Sheha, M.; Mohammadi, K.; Powell, K. Solving the Duck Curve in a Smart Grid Environment Using a Non-Cooperative Game Theory and Dynamic Pricing Profiles. *Energy Convers. Manag.* **2020**, *220*, 113102. [CrossRef]
34. NASA. NASA Data Access Viewer. Available online: https://power.larc.nasa.gov/data-access-viewer/ (accessed on 31 May 2024).
35. Brihmat, F.; Mekhtoub, S. PV Cell Temperature/PV Power Output Relationships Homer Methodology Calculation. In Proceedings of the Conférence Internationale des Energies Renouvelables, Sousse, Tunisia, 15–17 December 2013.
36. Kumar, P.P.; Suresh, V.; Jasinski, M.; Leonowicz, Z. Off-grid Rural Electrification in India Using Renewable Energy Resources and Different Battery Technologies with a Dynamic Differential Annealed Optimization. *Energies* **2021**, *14*, 5866. [CrossRef]
37. Hoppecke. Hoppecke Sun Power VR M Brochure. Available online: https://www.hoppecke.com/fileadmin/Redakteur/Hoppecke-Main/Products-Import/sun_power_vrm_brochure_en.pdf (accessed on 30 December 2024).
38. SMA. SUNNY ISLAND 4.4M/6.0H/8.0H Datasheet. Available online: https://files.sma.de/downloads/SI44M-80H-13-DS-en-31.pdf (accessed on 7 July 2024).
39. VHK and ARMINES. *Ecodesign & Labelling Review Household Refrigeration: Preparatory/Review Study—Commission Regulation (EC) No. 643/2009 and Commission (Delegated) Regulation (EU) 1060/2010*; Van Holsteijn en Kemna B.V.: Delft, Netherlands & Association pour la Recherche et le Développement des Méthodes et Processus Industriels: Paris, France, 2015. Available online: https://ecodesign-fridges.eu/sites/ecodesign-fridges.eu/files/HouseholdRefrigerationReviewTASK1_6DRAFTREPORT20151114.pdf (accessed on 8 December 2024).
40. Delgado-Sanchez, J.M.; Lillo-Bravo, I. Influence of Degradation Processes in Lead-Acid Batteries on the Technoeconomic Analysis of Photovoltaic Systems. *Energies* **2020**, *13*, 4075. [CrossRef]
41. Opiyo, N.N. Modelling Temporal Diffusion of PV Microgeneration Systems in a Rural Developing Community. Ph.D. Thesis, University of Leeds, Leeds, UK, 2016.

42. Ouédraogo, S.; Faggianelli, G.A.; Pigelet, G.; Notton, G.; Duchaud, J.L. Performances of Energy Management Strategies for a Photovoltaic/Battery Microgrid Considering Battery Degradation. *Sol. Energy* **2021**, *230*, 654–665. [CrossRef]
43. Ya'acob, N.; Apandi, A.S.G.A.; Yuso, A.L.; Kassim, M.; Naim, N.F. Prediction of Battery Lifetime Using Hybrid Solar Power System. *Math. Stat. Eng. Appl.* **2022**, *71*, 208–224. [CrossRef]

Disclaimer/Publisher's Note: The statements, opinions and data contained in all publications are solely those of the individual author(s) and contributor(s) and not of MDPI and/or the editor(s). MDPI and/or the editor(s) disclaim responsibility for any injury to people or property resulting from any ideas, methods, instructions or products referred to in the content.